

Wind-up in lamina I spinoparabrachial neurons: a role for reverberatory circuits

Junichi Hachisuka^{a,b}, Yu Omori^{a,b}, Michael C. Chiang^{a,b}, Michael S. Gold^{a,b}, H. Richard Koerber^{a,b}, Sarah E. Ross^{a,b,*}

Abstract

Wind-up is a frequency-dependent increase in the response of spinal cord neurons, which is believed to underlie temporal summation of nociceptive input. However, whether spinoparabrachial neurons, which likely contribute to the affective component of pain, undergo wind-up was unknown. Here, we addressed this question and investigated the underlying neural circuit. We show that one-fifth of lamina I spinoparabrachial neurons undergo wind-up, and provide evidence that wind-up in these cells is mediated in part by a network of spinal excitatory interneurons that show reverberating activity. These findings provide insight into a polysynaptic circuit of sensory augmentation that may contribute to the wind-up of pain's unpleasantness.

Keywords: Wind-up, Nociception, Neurotensin, Optogenetics, Spinal cord, Dorsal horn

1. Introduction

Wind-up is a type of facilitation observed in spinal cord neurons in which the response to repetitive stimulation of peripheral C-fibers increases with each stimulus.¹⁸ This mechanism of amplification was first described over 50 years ago in lamina IV spinocervical neurons, where it was shown to be a frequency-dependent phenomenon.^{22,23} Since then, this form of amplification has been observed in a variety of spinal neurons, including wide-dynamic-range (WDR) neurons in the deep dorsal horn, unidentified neurons in the superficial dorsal horn, and motor neurons in the ventral horn.^{36,49,50}

It has long been speculated that wind-up could contribute to the sensory experience of temporal summation, the increase in the perception of pain in response to repeated stimulation.^{2,8} Consistent with this possibility, temporal summation in response to electrical, thermal, or mechanical stimulation, is frequency dependent, and requires stimulus intensities capable of activating C-fibers.^{1,3,20,21,45} Both wind-up and temporal summation are physiological mechanisms of amplification that has the potential to contribute to hypersensitivity and allodynia after injury, as suggested by the observations that wind-up is magnified in mice with peripheral inflammation,^{17,18,40,43} and temporal summation is heightened in patients with pain.^{12,26,31,44} Thus, understanding the neural circuits

of wind-up is important because these circuits may contribute to pathological pain.^{11,47}

Although wind-up has been studied extensively, there remain 2 major unanswered questions. The first pertains to the affective component of pain. Many earlier studies have focused on amplification of reflexes, using wind-up in the ventral horn and/or motor roots as a primary endpoint with which to tease apart mechanisms underlying this phenomenon.^{30,36,49} Wind-up also occurs in spinal output neurons that project, directly or indirectly to the thalamus, such as WDR spinothalamic neurons⁵⁰ and spinocervical neurons.^{22,23} Because somatosensory input to the thalamus contributes to sensory discrimination, wind-up in these cells could account for the psychophysical phenomenon of temporal summation as manifest by reports of increasing pain intensity with repeated application of a noxious stimulus.²⁰ What remains unclear is whether there is wind-up in sensory affective pathways that mediate the unpleasantness of pain. Spinal output neurons that target the lateral parabrachial nucleus, which convey nociceptive and thermoregulatory information, are believed to contribute to the affective component of pain.^{5,14} However, whether wind-up occurs in spinoparabrachial (SPB) neurons is unknown. Given that pain unpleasantness shows temporal summation,³⁵ we hypothesized that wind-up would occur in SPB neurons.

The second unresolved question is whether synaptic mechanisms alone are sufficient to account for wind-up. The prevailing theory is that wind-up is mediated by *N*-methyl-D-aspartate (NMDA) receptors, which are recruited through a relief of magnesium block that occurs on cumulative depolarization in response to repetitive stimulation.⁸ A key role of NMDA receptors in wind-up is supported by the findings that NMDA receptor antagonists inhibit wind-up of WDR neurons,^{7,9} ventral horn neurons,⁴¹ and motor neurons.⁴⁸ Accordingly, NMDA receptor antagonists also reduce temporal summation in healthy humans^{2,32} and abnormal temporal summation in the context of injury-induced pain.^{13,46} However, the block of wind-up by NMDA receptor antagonists is not always complete, raising the possibility that other mechanisms are likely to contribute.^{7,9,41}

One possibility is a circuit-based mechanism in which an excitatory interneuron network in the dorsal horn acts as an

Sponsorships or competing interests that may be relevant to content are disclosed at the end of this article.

H.R. Koerber and S.E. Ross contributed equally to this work.

^a Department of Neurobiology, University of Pittsburgh, Pittsburgh, PA, United States, ^b Pittsburgh Center for Pain Research, University of Pittsburgh, Pittsburgh, PA, United States. Dr. Omori is now with the Toray Industries, Inc, Pharmaceutical Research Laboratories, Kamakura, Kanagawa, Japan

*Corresponding author. Address: 200 Lothrop St., W1456 BST, Department of Neurobiology, Pittsburgh Center for Pain Research, University of Pittsburgh, Pittsburgh, PA 15213. Tel.: +1 412-624-9178; fax: 412-648-1441. E-mail address: saross@pitt.edu (S.E. Ross).

PAIN 159 (2018) 1484–1493

© 2018 International Association for the Study of Pain

<http://dx.doi.org/10.1097/j.pain.0000000000001229>

amplifier. Indeed, such a circuit-based mechanism was originally put forth by Mendell in his seminal study, in which he postulated that wind-up may be due to the reverberatory activity in spinal interneurons that is evoked by afferent C-fiber input, reasoning that “if in this period of time another stimulation arrives to the cord, it sums with the ongoing activity to produce a more intense discharge in the interneurons than the one before it²².” Consistent with this idea, wind-up is observed in a variety of spinal neurons that do not receive appreciable C-fiber input, indicating that this wind-up must be mediated through a polysynaptic circuit. However, the nature of this circuit, and whether it contributes to (rather than simply propagating) wind-up is not clear.

We recently developed an *ex vivo* somatosensory preparation that enables the recording from lamina I SPB neurons together with cell-type-specific manipulation.¹⁶ We therefore set out to test the hypotheses that wind-up occurs in lamina I SPB neurons, and that a network of excitatory interneurons is involved in mediating this amplification. Here, we report that approximately one-fifth of SPB neurons show wind-up on repetitive stimulation of the dorsal root. In addition, we provide evidence that optogenetic activation of excitatory interneurons is sufficient for wind-up. This effect is selective for some excitatory networks because it is observed on activation neurons of the neurotensin-lineage (Nts^{Cre}) neurons but not the calretinin lineage (Cr^{Cre}) neurons. Through optogenetic inhibition, we show that activity in Nts^{Cre} neurons is required for dorsal root-evoked wind-up. Finally, our data suggest that this facilitation is mediated, at least in part, by reverberatory activity within an interconnected excitatory network. Together, these studies show the existence of wind-up in lamina I SPB neurons and provide new insight into the underlying neural circuit basis.

2. Methods

2.1. Mouse lines

The mouse lines used for this study were all obtained from The Jackson Laboratories and maintained on C57BL/6J background: Nts^{Cre}, a nondisruptive IRES-Cre recombinase knock-in at the endogenous Neurotensin locus (Stock number: 017525); Cr^{Cre}, a nondisruptive IRES-Cre recombinase knock-in at the endogenous Calretinin locus (Stock number: 010774); Ai9, enabling Cre-dependent expression of tdTomato (*Gt(ROSA)26Sor^{tm9(CAG-tdTomato)}*, Stock number: 007909); Ai32, enabling Cre-dependent expression of an enhanced channelrhodopsin fusion protein, ChR2(H134)/EYFP (*Gt(ROSA)26Sor^{tm32(CAG-COP4*H134R/EYFP)}*, Stock number: 012569); and Ai35, enabling Cre-dependent expression of an Archaelhodopsin fusion protein (*Gt(ROSA)26Sor^{tm35.1(CAG-aop3/GFP)}*; Stock number: 012735). Genotyping for these alleles was performed with the following primers: for Ai9, TdTR (GGC ATT AAA GCA GCG TAT CC) and TdTR (CTG TTC CTG TAC GGC ATG G) were used to detect TdTomato (196 bp product); for Ai32, ChR2F (ACA TGG TCC TGC TGG AGT TC) and ChR2R (GGC ATT AAA GCA GCG TAT CC) were used to detect ChR2 (212 bp product); for Ai35, XFPP (GCG AGG GCG AGG GCG ATG) and XFPR (CGA TGT TGT GGC GGA TCT TG) were used to detect EYFP (423 bp product), and for the wild-type Rosa allele, RosaWTF (GGA GCG GGA GAA ATG GAT ATG) and RosaWTR (AAA GTC GCT CTG AGT TGT TAT) were used (~550 bp product).

Four- to seven-week-old mice of both sexes were used in this study. Mice were given free access to food and water and housed under standard laboratory conditions. The use of animals was approved by the Institutional Animal Care and Use Committee of the University of Pittsburgh.

2.2. Immunohistochemistry

Four Nts^{Cre}; *Gt(ROSA)26Sor^{tm9(CAG-tdTomato)}* adult mice were perfused with 4% paraformaldehyde and the lumbar spinal cords from L2 to L3 were dissected and subsequently postfixed for 4 hours. Transverse 65- μ m thick sections were cut on a vibrating microtome and processed free-floating for immunohistochemistry. Sections were blocked in blocking solution (10% donkey serum, 0.1% Triton in phosphate-buffered saline) for 2 hours and incubated in the following primary antibodies for 14 hours overnight at 4°C: NeuN (1:1000 Millipore MAB377; Millipore, Burlington, MA) and Pax2 (1:1000, Life Technologies 716000; Life Technologies, Carlsbad, CA) as well as Biotin-conjugated Isolectin B4 (1:200, Sigma Aldrich L2140; Sigma Aldrich, St. Louis, MO). After three 20-minute washes with wash buffer (0.1% Triton, 1% donkey serum, 0.3 M NaCl), sections were incubated with Alexa Fluor-conjugated secondary antibodies (1:500; Life Technologies) and Streptavidin-488 (1:500; Thermo Fisher, Waltham, MA) and for 2 hours at room temperature. Next, sections were incubated with Hoechst (1:10,000; Thermo Fisher) incubation for 1 minute to label nuclei. Seven 15-minute washes were performed, and then, sections were mounted on slides and coverslipped. The dorsal horns were imaged through a single optical plane using a Nikon A1R confocal microscope with a 20 \times objective. Only cells with clearly visible nuclei were counted.

2.3. Labeling spinoparabrachial neurons

Four- to six-week-old mice were anesthetized with isoflurane and placed in a stereotaxic frame. A small hole was made on the skull with dental drill. A glass micropipette was used to inject 100 nL of FAST Dil oil (2.5 mg/mL; Invitrogen, Carlsbad, CA) into left lateral parabrachial nucleus (relative to lambda: anteroposterior – 0.5 mm; lateral 1.3 mm; and dorsoventral –2.4 mm). The head wound was closed with stitches. After recovery from the anesthesia, the animals fed and drank normally. The animals were used for electrophysiology 4 to 7 days later.

2.4. Whole spinal cord preparation

For electrophysiological recordings, we used a modified semi-intact preparation.¹⁶ We recorded from neurons in the L2 spinal segment, which are easiest to visualize and record from in this preparation. In brief, 5- to 7-week-old mice were deeply anesthetized with urethane (1.2 g/kg, intraperitoneally). The animals were perfused transcardially through the left ventricle with ice-cold oxygenated (95% O₂ and 5% CO₂) sucrose-based artificial cerebrospinal fluid (in mM; 234 sucrose, 2.5 KCl, 0.5 CaCl₂, 10 MgSO₄, 1.25 NaH₂PO₄, 26 NaHCO₃, and 11 glucose). Immediately after perfusion, the skin was incised along the dorsal midline and the spinal cord was quickly excised and placed into an ice-cold, sucrose-based Krebs solution. Dura and pia-arachnoid membrane were removed after cutting all the ventral and dorsal roots except the L2 root on the right. The spinal cord was placed in the recording chamber and pinned into a chamber wall made from Sylgard. The spinal cord was perfused with Krebs solution saturated with 95% O₂ and 5% CO₂ at 30 to 31°C. The Krebs solution contained (mM): 117 NaCl, 3.6 KCl, 2.5 CaCl₂, 1.2 MgCl₂, 1.2 NaH₂PO₄, 25 NaHCO₃, and 11 glucose.

2.5. Patch-clamp recording from dorsal horn neurons

Neurons were visualized using a fixed stage upright microscope (BX51WI Olympus microscope; Olympus, Tokyo, Japan) equipped with a 40 \times water immersion objective lens, a CCD camera

(ORCA-ER; Hamamatsu Photonics, Hamamatsu City, Japan), and monitor screen. A narrow beam infrared LED (L850D-06; Marubeni, Tokyo, Japan, emission peak, 850 nm) was positioned outside the solution meniscus, as previously described.^{16,28,29,34} To record from Nts^{Cre} neurons in optogenetic experiments, mice were generated that harbored both Ai14 and Ai32 alleles, and cells were identified by expression of tdTomato. Spinoparabrachial neurons located within 20 μ m from the surface of the dorsal horn were identified by Dil labeling.

Whole-cell patch-clamp recordings were made with an Axopatch 200B amplifier with a Digidata 1322A A/D converter controlled using Clampex software (version 10), all from Molecular Devices. Patch-pipette electrodes had a resistance of 6 to 12 M Ω when filled with a pipette solution of the following composition (mM): 135 potassium gluconate, 5 KCl, 0.5 CaCl₂, 5 EGTA, 5 Hepes, 5 ATP-Mg, pH 7.2. Alexa Fluor 488 was added to aid in visualization. The data were low-pass filtered at 2 kHz and digitized at 10 kHz. The liquid junction potential was not corrected.

Cell recordings were made in voltage-clamp mode at holding potentials of -70 mV to record excitatory postsynaptic currents (EPSCs) and current-clamp mode to record action potentials (APs). Frequency of EPSCs and APs was analyzed using MiniAnalysis (Synaptosoft, Inc, Decatur, GA). The L2 dorsal root was stimulated by suction electrode with 100 ms duration. Ad-fiber evoked responses were considered monosynaptic if the latency remained constant when the root was stimulated at 20 Hz and there was no failure, and C-fiber evoked responses were considered monosynaptic if there was no failure at 2 Hz.²⁵ To investigate wind-up, dorsal root stimulation (DRS) was applied at 2 Hz and the number of APs after each stimulation (0.5-second window) was counted. The criteria used to define the presence of wind-up were that the maximum number of APs was at least 5 and more than twice as many APs were evoked in response to subsequent stimuli as were evoked in response to the first stimulus.

2.6. Optogenetic activation

During patch-clamp recording, photostimulation was applied to the spinal cord through the objective lens (40 \times) of the microscope with a Xenon lamp (Lambda DG-4; Sutter Instrument, Novato, CA). A Lambda DG4 (Sutter Instrument) was used for optogenetic stimulation, where switching between filter positions (0.5 ms) was controlled by a TTL pulse from the output of the A/D converter. We used a GFP filter (centered around 485 nm) for activation of ChR2 and a Cy3 filter (centered around 555 nm) for activation of Arch. Light power on the sample was 1.3 mW/mm². To examine whether the recorded neuron received monosynaptic or polysynaptic input from Nts^{Cre} neurons, we applied 0.1-Hz photostimulation (5 ms). Input was considered monosynaptic if there was no failure and the latency jitter was smaller than 1 ms.¹⁶ For blue light-induced wind-up, we applied 2-Hz photostimulation (5 ms), using the same wind-up criteria as root-evoked wind-up. To test whether activation of Nts^{Cre} primary afferents caused wind-up, blue light pulse of the same light source was applied on the dorsal root, which was approximately 7 mm away from the spinal cord and far enough to prevent blue light-induced ChR2 activation in the spinal cord.

3. Results

3.1. Dorsal root stimulation induces wind-up in one-fifth of lamina I spinoparabrachial neurons

To determine whether wind-up develops in SPB neurons, we used an ex vivo spinal cord preparation that preserves intact

spinal circuitry and enables whole-cell recordings from SPB neurons in lamina I (**Figs. 1A and B**), as described previously.¹⁶ After the injection of Dil into the lateral parabrachial nucleus, retrogradely labeled lamina I SPB neurons were identified for recording with epifluorescence and then visualized in bright field by oblique infrared LED illumination to establish whole-cell patch recording (**Fig. 1C**).^{16,39}

Electrical stimulation of L2 dorsal root at 0.5 Hz, elicited a stable response to each stimulus in most cases (**Fig. 1D**, bottom and **Fig. 1E**, black trace). However, at 2 Hz stimulation, there was a progressive increase in AP number across the period of stimulation in 12 of 67 lamina I SPB neurons studied (**Fig. 1D**, top and **Fig. 1E**, red trace). In these neurons, there was a $299 \pm 70\%$ increase in the maximum number of evoked APs by the end of the 10-pulse train relative to the number of APs evoked with the first pulse. This effect was in marked contrast to the absence of a change in the number of evoked APs ($6 \pm 11\%$) in the remaining neurons (**Fig. 1F**). Importantly, and consistent with previous characterizations of wind-up, the increase in the evoked response to DRS significantly reduced by the NMDA receptor antagonist APV (50 μ M; **Fig. 1G**). Thus, wind-up is observed in $\sim 20\%$ of lamina I SPB neurons and, like in other spinal neurons, it is NMDA receptor dependent.

3.2. Neurotensin-lineage neurons are sufficient for wind-up in lamina I spinoparabrachial neurons

To identify spinal neurons potentially underlying the reverberating circuit hypothesized by Mendell,²² we screened for Cre alleles that would enable genetic access to subsets of excitatory neurons. The Nts^{Cre} allele was selected because it is relatively specific for excitatory interneurons and it targets a broad population in the dorsal horn. To determine the distribution of these cells, we analyzed L2 to L3 spinal dorsal horns from mice harboring both the Nts^{Cre} and the Ai14 tdTomato reporter alleles, which were costained for NeuN, a marker of neurons, Pax2, a marker of inhibitory neurons, and IB4, a marker of non-peptidergic afferents that were used to help delineate boundaries within the dorsal horn. Using the ventral aspect of IB4 as a boundary that corresponds approximately to the border between high-threshold C-fiber and low-threshold A-fiber inputs, we found that Nts^{Cre} neurons represent $13 \pm 1\%$ of neurons within the superficial dorsal horn and $32 \pm 2\%$ of neurons within the intermediate dorsal horn ($n = 4$ mice). Almost all ($98 \pm 1\%$) the Nts^{Cre} neurons were deemed to be excitatory as evidenced by the absence of Pax2 staining (**Fig. 2A**).^{6,30} Because the genetic population defined by Nts^{Cre}-mediated recombination is somewhat broader than that defined by neurotensin protein expression in adult mice,¹⁵ we refer to the Nts^{Cre} population as neurotensin-lineage neurons.

Because we wanted to know whether stimulation of Nts^{Cre} neurons alone was sufficient to drive wind-up in lamina I SPB neurons, it was first necessary to confirm that we could consistently activate Nts^{Cre} neurons expressing ChR2 with blue light (**Fig. 2B**). We found that brief (5 ms) blue light exposure typically induced 1 AP in ChR2-expressing Nts^{Cre} neurons, which could follow at 2 Hz (**Fig. 2C**) with a failure rate of less than 5% ($4 \pm 3\%$, $n = 16$ cells).

Having confirmed that it was possible to selectively activate Nts^{Cre} neurons, we next sought to determine whether selective activation of these neurons was sufficient to drive wind-up in lamina I (**Fig. 2D**). For the sake of ease in this preliminary screen, we analyzed unidentified lamina I neurons (rather than

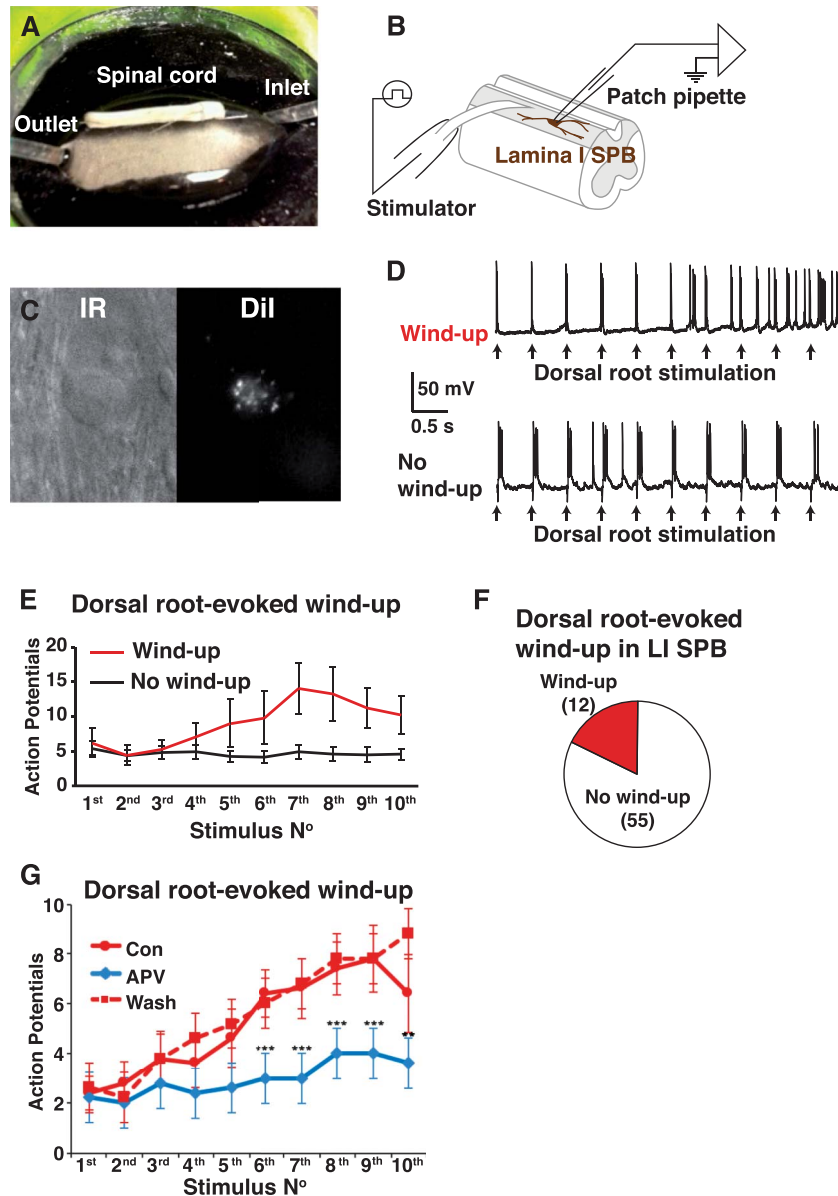


Figure 1. Dorsal root stimulation induces wind-up in 18% of lamina I SPB neurons. (A and B) Photograph (A) and schematic (B) of recording setup in whole spinal cord preparation. Whole-cell patch-clamp recording was made from the lamina I SPB neurons. (C) Infrared (IR) and fluorescent image of a lamina I SPB neuron that is labeled with Dil. (D) Example traces of wind-up and no wind-up in response to 2 Hz dorsal root stimulation. (E) Wind-up is observed in a subset of lamina I SPB neurons in response to 2 Hz root stimulation. (F) Pie chart illustrating fraction of lamina I SPB neurons that show wind-up. (G) Treatment with the NMDA antagonist APV (50 μ M) significantly reduced wind-up in lamina I SPB neurons in response to 2 Hz root stimulation, which recovered on wash. Data are mean \pm SEM ($n = 5$ cells, paired; asterisks indicate significantly different than control, ** $P < 0.01$, *** $P < 0.001$, 2-way ANOVA followed by the Dunnett multiple comparison test). ANOVA, analysis of variance; LI, lamina I; NMDA, *N*-methyl-D-aspartate; SPB, spinoparabrachial.

retrogradely labeled SPB neurons). Optogenetic stimulation at 2 Hz caused a robust wind-up in 6 of 9 neurons (Figs. 2E and F), indicating that Nts^{Cre} interneuron activity is sufficient for wind-up. To determine whether optogenetically induced wind-up by excitatory neurons in the dorsal horn occurs in response to the stimulation of any excitatory neuron subpopulation, we assessed the impact of optogenetic stimulation of Cr^{Cre} neurons (Fig. 2G). Calretinin is expressed in \sim 30% of neurons in the superficial dorsal horn, of which 85% are excitatory.^{37,38} Although optogenetically evoked APs were observed in lamina I neurons on application of blue light, wind-up was not detected on activation of Cr^{Cre} neurons (Figs. 2H and I). Thus, the selective activation of some, but not all, excitatory neurons is sufficient to induce wind-up in lamina I neurons.

Next, we turned to the analysis of lamina I SPB neurons because these output neurons may be involved in the affective component of pain. Notably, although some of the input from primary afferents onto lamina I SPB neurons is direct, the majority occurs through polysynaptic connections (Figs. 3A and B), raising the possibility that an excitatory network could contribute to wind-up in lamina I SPB neurons. To test this possibility, we examined the effect of optogenetic stimulation of Nts^{Cre} neurons (Fig. 3C). Blue light stimulation of Nts^{Cre} neurons at 2 Hz caused wind-up in 11 of 18 (61%) lamina I SPB neurons (Figs. 3D and E). Thus, optogenetically induced wind-up was observed in a significantly larger population of lamina I SPB neurons than dorsal root–evoked wind-up ($P < 0.01$, Fisher exact test). In some neurons, the peak response to the wind-up protocol was achieved by the sixth or seventh stimulus in the train,

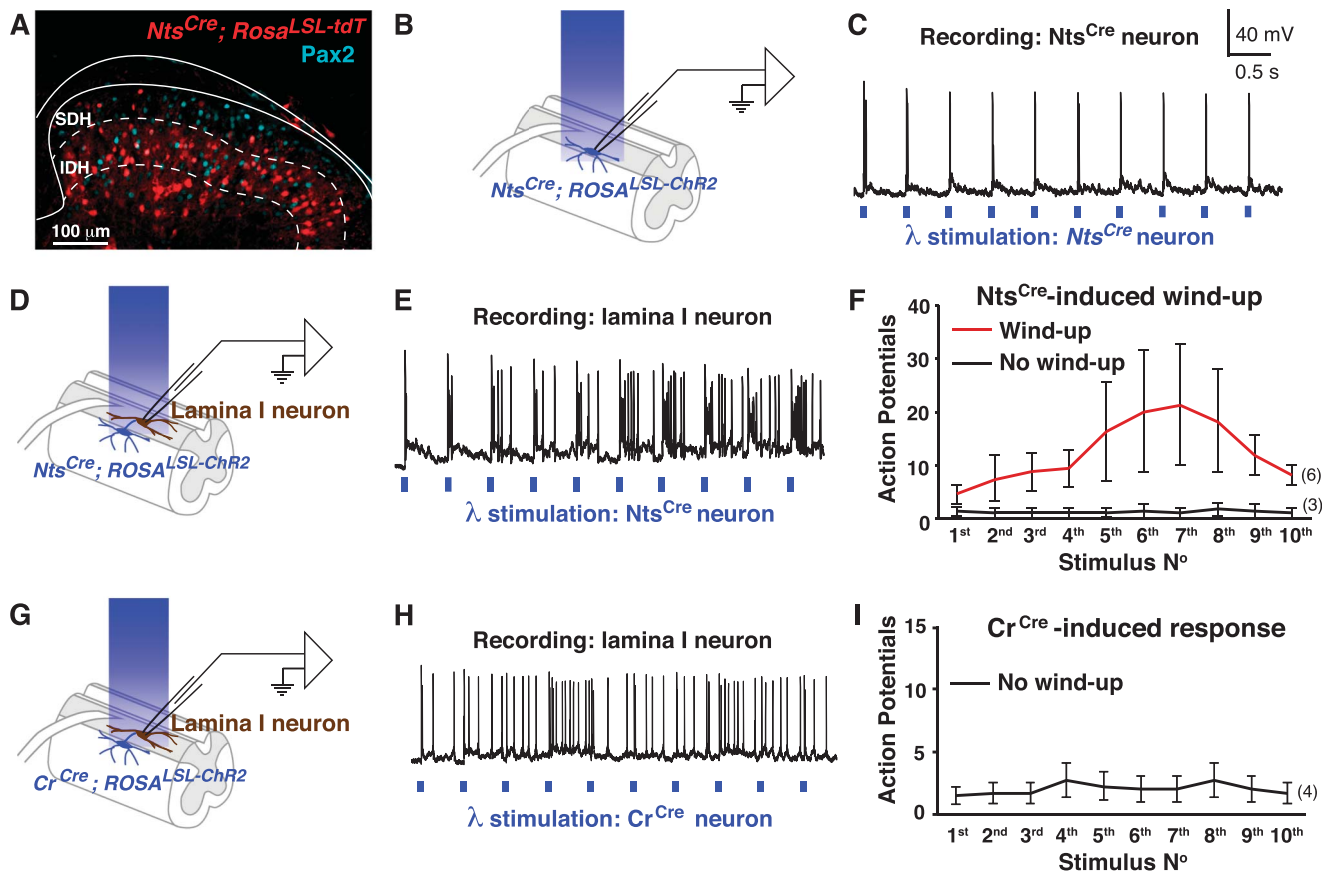


Figure 2. Activation of excitatory neurons can induce wind-up in lamina I. (A) Spinal cord sections (L2–L3) from adult *Nts^{Cre}; ROSA^{LSL-tdT}* mice were immunostained to reveal the inhibitory marker Pax2 (green). The vast majority of tdTomato-labeled *Nts^{Cre}* neurons are Pax2-negative. (A) Single confocal optical section of the dorsal horn is shown. For quantification, the ventral border of the IB4 binding (not shown) was used to demarcate the lower boundary of the superficial dorsal horn (SDH); a second boundary, 85 μ m below the first, was used to demarcate the intermediate dorsal horn (IDH). (B) Schematic of optogenetic stimulation and whole-cell patch-clamp recording from the *Nts^{Cre}; ROSA^{LSL-ChR2}* neuron. (C) Optogenetic stimulation (5 ms) evoked APs in an *Nts^{Cre}* neuron, which could follow at 2 Hz. (D) Schematic of optogenetic stimulation and whole-cell patch-clamp recording from an unidentified lamina I neuron from *Nts^{Cre}; ROSA26^{LSL-ChR2}* mice. (E and F) Optogenetic stimulation of *Nts^{Cre}* neurons at 2 Hz caused wind-up in 6 of 9 lamina I neurons; example trace (E) and summary (F). Data are mean \pm SEM. (G) Schematic of optogenetic stimulation and whole-cell patch-clamp recording from an unidentified lamina I neuron from *Cr^{Cre}; ROSA26^{LSL-ChR2}* mice. (H and I) Optogenetic stimulation of *Cr^{Cre}* neurons at 2 Hz causes APs in lamina I neurons, but no wind-up ($n = 4$ cells); example trace (H) and summary (I). Data are mean \pm SEM. AP, action potential.

with a decrease from this peak response observed to the remaining stimuli (Fig. 3D). We suggest that this decrease may be due to a depolarization-induced inactivation of voltage-gated sodium channels. Like dorsal root-evoked wind-up, the *Nts^{Cre}*-mediated wind-up of lamina I SPB neurons was blocked by APV (Fig. 3F) and showed frequency dependence (Figs. 3G and H).

An important consideration is that, in addition to excitatory spinal interneurons, the *Nts^{Cre}* allele causes recombination in approximately 10% of primary afferents, which are mainly small diameter cells, and include both peptidergic and nonpeptidergic subtypes (data not shown). To address the potential role of *Nts^{Cre}* primary afferents in optogenetically induced wind-up, we compared the responses of a given lamina I SPB neuron to optogenetic stimulation over the cord (Fig. 3C) with that observed over the root (Fig. 3I). As before, optogenetic stimulation over the cord induced wind-up (Fig. 3K). By contrast, optogenetic stimulation of the *Nts^{Cre}* afferent input was not sufficient for wind-up in lamina I SPB neurons, although in all cases it was sufficient to drive APs in these cells (Figs. 3J and K). Thus, although we cannot rule out a possible contribution from primary afferents, wind-up in lamina I SPB neurons by optogenetic activation of the *Nts^{Cre}* population likely requires activity in neurotensin-lineage neurons in the dorsal horn.

3.3. Neurotensin-lineage neurons are required for wind-up in lamina I spinoparabrachial neurons

Although activation of the local *Nts^{Cre}* network is sufficient for wind-up in lamina I SPB neurons, whether the *Nts^{Cre}* network normally mediates wind-up that is observed on electrical stimulation of C-fibers remained unclear. To address this question, we examined whether dorsal root-evoked wind-up is abolished on optogenetic inhibition of neurotensin-lineage neurons with Arch, a light-driven proton pump. To determine whether green light-induced activation of Arch was sufficient to inhibit *Nts^{Cre}* neurons, we recorded from these neurons in voltage and current clamp (Fig. 4A). Green light hyperpolarized Arch-expressing *Nts^{Cre}* neurons (10.3 ± 1.4 mV, $n = 13$ cells) and blocked dorsal root-evoked APs in these cells (Figs. 4B and C), thereby confirming the efficacy of this optogenetic strategy. Next, we addressed whether optogenetic inhibition of *Nts^{Cre}* neurons blocked root-evoked wind-up in lamina I SPB neurons. Towards this end, we identified lamina I SPB neurons that showed wind-up on electrical stimulation of the dorsal root and then, we repeated the stimulation in the presence of green light to inhibit *Nts^{Cre}* neurons (Fig. 4D). We found that optogenetic inhibition of *Nts^{Cre}* neurons significantly reduced root-evoked wind-up (Figs. 4E and F). To gain insight into

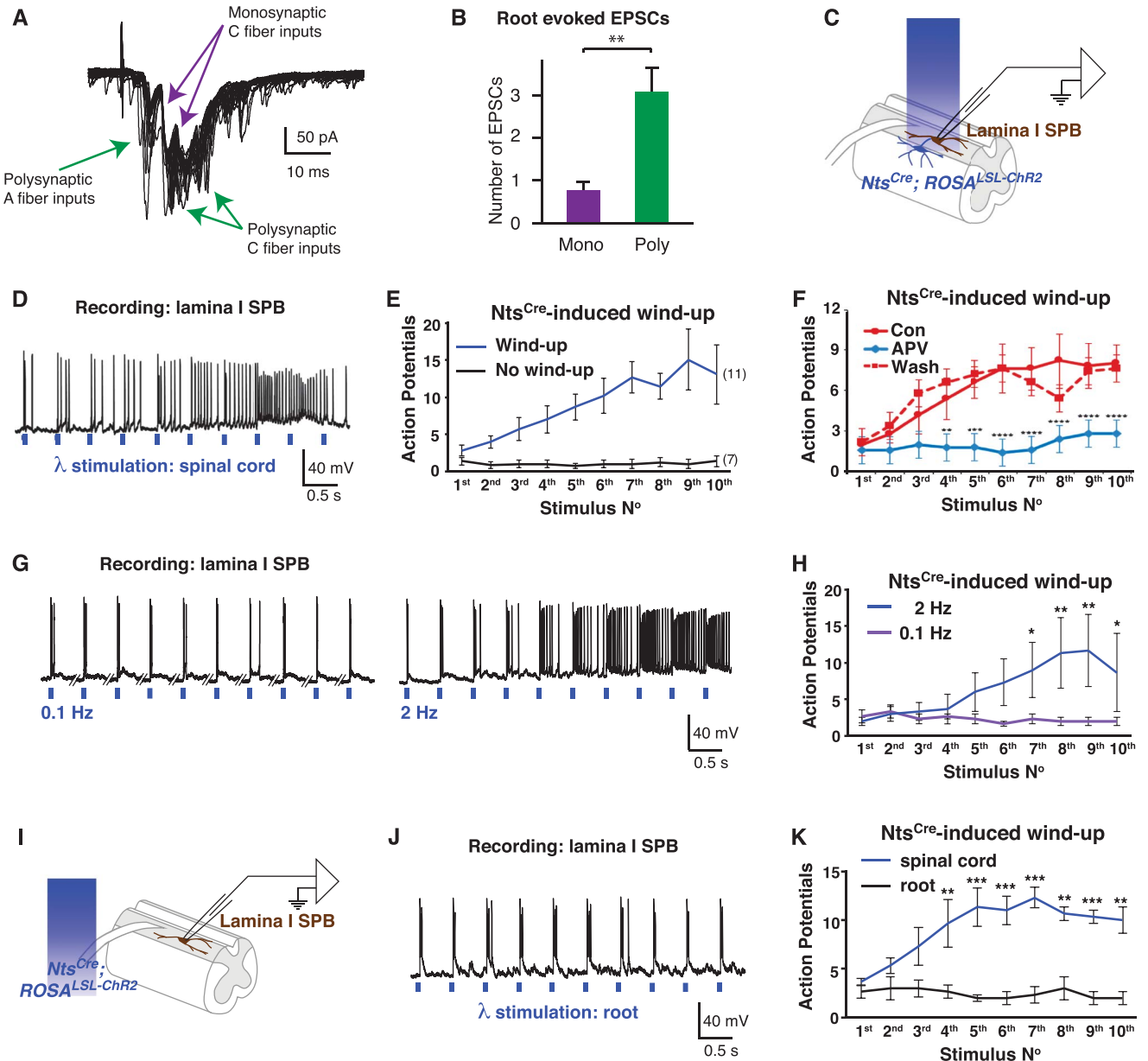


Figure 3. Activation of *Nts^{Cre}* neurons induced wind-up in lamina I SPB neurons. (A) Example traces of dorsal root-evoked EPSCs by 2 Hz dorsal root stimulation. Purple arrows indicate likely monosynaptic EPSCs, which have no failure and small jitter. Green arrows indicate polysynaptic EPSCs that have failures or large latency jitter. (B) Number of likely monosynaptic EPSCs and polysynaptic EPSCs observed on dorsal root stimulation. Data are mean \pm SEM (n = 13 cells, $**P < 0.01$, paired *t* test). (C) Schematic of optogenetic stimulation and whole-cell patch-clamp recording from a lamina I SPB neuron from *Nts^{Cre}; ROSA^{LSL-ChR2}* mice. (D and E) Optogenetic stimulation of *Nts^{Cre}* neurons at 2 Hz induced wind-up in 11 of 18 lamina I SPB neurons; example trace (D) and summary (E). Data are mean \pm SEM. (F) Treatment with APV (50 μ M) significantly reduced wind-up by 2 Hz stimulation of *Nts^{Cre}* neurons, which recovered on wash. Data are mean \pm SEM (n = 5 cells, paired; asterisks indicate significantly different than control, $**P < 0.001$, $***P < 0.001$, $****P < 0.0001$, 2-way ANOVA followed by the Dunnett multiple comparison test). (G–H) Optogenetically induced wind-up in lamina I SPB neurons occurs on stimulation at 2 Hz, but not 0.1 Hz; example trace (G) and summary (H). Data are mean \pm SEM (n = 3 cells, paired; $*P < 0.01$, $**P < 0.01$, 2-way ANOVA followed by the Bonferroni post hoc test). (I) Schematic of optogenetic stimulation of the dorsal root and whole-cell patch-clamp recording from a lamina I SPB neuron. (J) Example trace illustrating that optogenetic stimulation of the dorsal root at 2 Hz does not evoke wind-up in lamina I SPB neurons. (K) Quantification of APs after 2 Hz optogenetic stimulation over the spinal cord (blue) or the dorsal root (black). Data are mean \pm SEM (n = 3 cells, paired; $**P < 0.01$, $***P < 0.001$, 2-way ANOVA followed by the Bonferroni post hoc test). ANOVA, analysis of variance; AP, action potential; EPSC, excitatory postsynaptic current; SPB, spinoparabrachial.

the underlying mechanism, we performed recordings in voltage clamp to analyze the effect of green light on the input received by lamina I SPB neurons. This analysis revealed that optogenetic inhibition of *Nts^{Cre}* neurons significantly reduced the excitatory input that is observed on dorsal root stimulation, as measured by the net influx of charge (Figs. 4G and H). Taken together, these findings suggest that activity in *Nts^{Cre}* neurons is required for dorsal root-evoked wind-up.

3.4. *Nts^{Cre}* neurons form an extensive excitatory network

Our results suggested that *Nts^{Cre}* neurons are necessary and sufficient for wind-up, but the underlying circuitry remained unclear. To address this, we analyzed ChR2-evoked currents in voltage-clamp mode. We found that, although a small proportion (2 of 30) of lamina I SPB neurons did not receive any input from *Nts^{Cre}* neurons (Fig. 5A), most showed either monosynaptic and polysynaptic EPSCs (16 of 30; Fig. 5B) or polysynaptic EPSCs (12 of 30; Fig. 5C).

Thus, most lamina I SPB neurons receive direct or indirect input from Nts^{Cre} neurons (Fig. 5D). Next, we examined the connectivity among Nts^{Cre} neurons, recording from Nts^{Cre} neurons while activating this population optogenetically. In 3 of 25 Nts^{Cre} neurons, optogenetic stimulation evoked only a single, large amplitude ChR2-evoked current with very short latency (~1 ms) because of the opening of ChR2 in the recorded cell (Fig. 5E). However, in most Nts^{Cre} neurons, this large amplitude ChR2-evoked current was accompanied by monosynaptic and polysynaptic EPSCs (Fig. 5F), or polysynaptic EPSCs (Fig. 5G). Together, these findings suggest that Nts^{Cre} neurons form an excitatory network.

3.5. Activation of Nts^{Cre} neurons causes reverberatory activity that correlates with wind-up

The extensive interconnectivity that we observed within the Nts^{Cre} network raised the possibility that a polysynaptic circuit

also contributes to the wind-up in lamina I SPB neurons. If so, we reasoned that we ought to see not only wind-up of the light-evoked EPSCs in lamina I SPB neurons but also an increase in the subsequent polysynaptic input onto these cells. To investigate this possibility, we recorded from lamina I SPB neurons in voltage-clamp mode in response to optogenetic activation of Nts^{Cre} neurons (Fig. 6A). Blue light stimulation at 2 Hz resulted in an increase in both the blue light-evoked EPSC and smaller EPSCs that followed, which seemed to be due to ongoing synaptic input onto the SPB neuron (Fig. 6B). To quantify this effect, we measured the net charge influx between stimuli. This analysis revealed that the net charge increase observed on repeated stimulation was significantly greater in cells that showed wind-up compared with cells that did not (Fig. 6C).

One of the factors that could lead to increased net charge influx is reverberatory activity within the network. We found

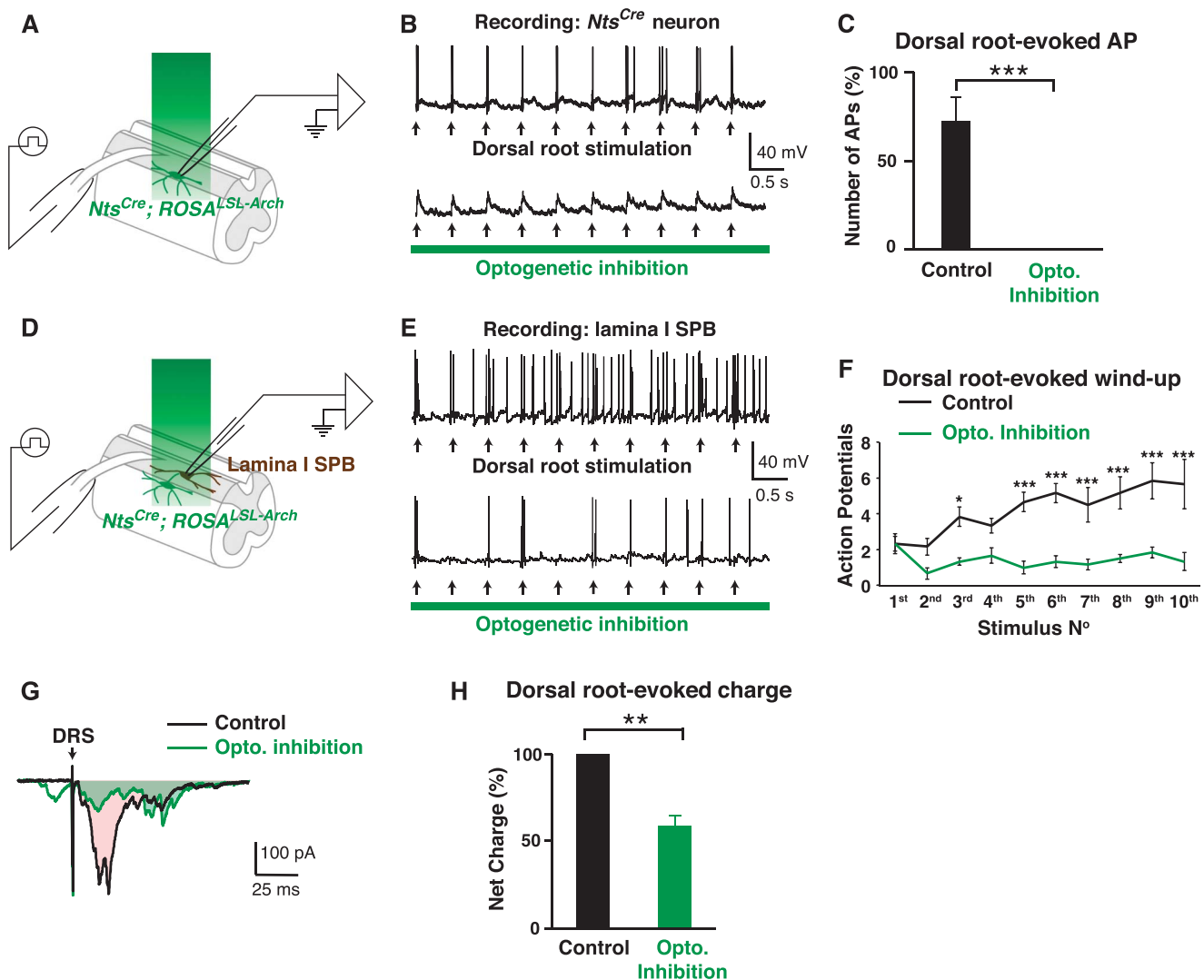


Figure 4. Inhibition of Nts^{Cre} neurons blocks dorsal root-evoked wind-up. (A) Schematic illustrating optogenetic inhibition and whole-cell patch-clamp recording from the $Nts^{Cre}; ROSA26^{LSL-Arch}$ neuron. (B and C) Optogenetic inhibition of Nts^{Cre} neurons blocks root-evoked action potentials in these cells, confirming effectiveness of optogenetic strategy; example traces (B) and quantification (C) Data are mean \pm SEM ($n = 5$ cells, $***P < 0.001$, paired t test). (D) Diagram illustrating optogenetic inhibition and whole-cell patch-clamp recording of a lamina I SPB neuron from $Nts^{Cre}; ROSA26^{LSL-Arch}$ mice. (E and F) Wind-up in lamina I SPB neurons elicited by dorsal root stimulation (DRS) was blocked on optogenetic inhibition of Nts^{Cre} neurons; example traces (E) and summary (F). Data are mean \pm SEM ($n = 5$ cells, paired, $*P < 0.05$, $**P < 0.01$, 2-way ANOVA followed by the Bonferroni post hoc test). (G) Example trace of evoked EPSCs after DRS in the absence (Control) or in the presence (Opto. Inhibition) of green light to inhibit Nts^{Cre} neurons. Shaded area represents under the curve represents charge. (H) Dorsal root-evoked charge, as measured by area under the curve, is significantly reduced on optogenetic inhibition of Nts^{Cre} neurons. Data are mean \pm SEM, normalized to control ($n = 5$ cells, paired; $**P < 0.01$; Student t test). ANOVA, analysis of variance; AP, action potential; EPSC, excitatory postsynaptic current; SPB, spinoparabrachial.

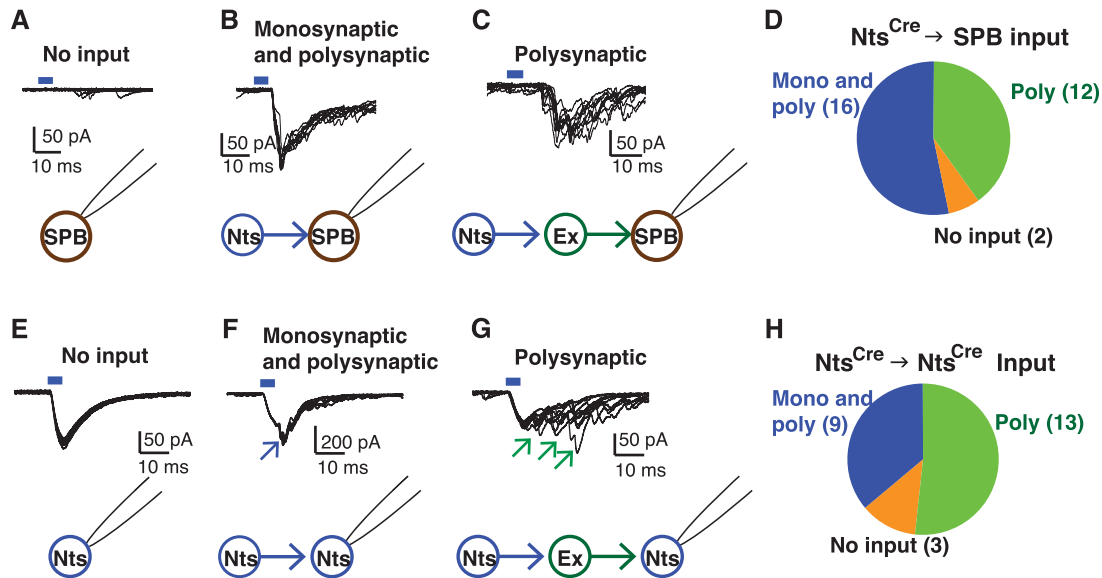


Figure 5. Nts^{Cre} neurons form an extensive excitatory network. (A–C) Whole-cell patch-clamp recording from lamina I SPB neurons on optogenetic stimulation of Nts^{Cre} neurons (0.1 Hz × 10, 5 ms duration). Example traces from recorded cells that received no input (A), monosynaptic and polysynaptic input (B), or polysynaptic input alone (C) from Nts^{Cre} neurons. (D) Summary data; n = 30 cells. (E–G) Whole-cell patch-clamp recording from Nts^{Cre} neurons on optogenetic stimulation of Nts^{Cre} neurons (0.1 Hz × 10, 5 ms duration). Example traces from recorded cells that received no input (E) (inward current is due to opening of ChR2 in the recorded cell), monosynaptic and polysynaptic input, as indicated by the blue arrow (F), or polysynaptic input alone, as indicated by the green arrows (G) from Nts^{Cre} neurons. (H) Summary data; n = 25 cells. SPB, spinoparabrachial.

that brief (5 ms) blue light stimulation induced EPSCs (Fig. 6D) that continued for the prolonged period (eg, > 1 second). Given the extended time course of this reverberatory activity, we reasoned that a second stimulus during this time could sum with previous activity, thereby contributing to wind-up as previously suggested.²² To test this idea, we compared the reverberating activity evoked by a single stimulus between lamina I SPB neurons that subsequently showed wind-up to those that did not. In this retrospective analysis, we found that in lamina I SPB neurons where no wind-up was observed, there was no difference in the EPSC frequency during the 1000 to 500 ms before optogenetic stimulation compared with the EPSC frequency during the 500 to 1000 ms after optogenetic stimulation. By contrast, in lamina I SPB neurons where wind-up was observed, there was a significant increase in the EPSC frequency observed after optogenetic stimulation compared with before (Figs. 6E and F). Together, these findings suggest that wind-up in lamina I SPB neurons is mediated, at least in part, by a polysynaptic circuit that shows reverberatory activity (Fig. 6G).

4. Discussion

Wind-up is a mechanism of facilitation that is believed to account for the intensification of pain observed with repeated or prolonged application of noxious stimuli, a psychophysical phenomenon referred to as temporal summation. Importantly, both the sensory/discriminative (intensity) and the emotional/affective (unpleasantness) components of pain are subject to temporal summation. Spinothalamic neurons, which are believed to contribute to intensity coding, undergo wind-up, but whether SPB neurons, which are believed to contribute to unpleasantness coding, are subject to wind-up, was less clear. Our study reveals that lamina I SPB neurons show wind-up in response to repetitive stimulation of the dorsal root. In addition, we provide evidence that this wind-up is mediated, at

least in part, by Nts^{Cre} neurons because selective activation of these cells was sufficient to evoke wind-up in lamina I SPB neurons, whereas optogenetic inhibition of these cells inhibited dorsal root-evoked wind-up. Finally, our data suggest that the duration of reverberatory input onto lamina I SPB neurons contributes to the manifestation of wind-up. These findings provide new insight into the circuit mechanisms that could underlie the temporal summation of pain's unpleasantness, and uncover a long-suspected contribution of an excitatory network in this sensory augmentation (Fig. 6E).

Our study reveals that wind-up in lamina I SPB neurons on optogenetic stimulation of Nts^{Cre} neurons was more frequent in occurrence than that observed on electrical stimulation of the dorsal root. Although the reason for this difference is not known, we suggest that the key role of inhibitory neurons within nociceptive circuits of the dorsal horn is likely to account for the difference. That is, primary afferent input normally recruits activity in inhibitory interneurons to effect feed-forward, feedback, and lateral inhibition. By contrast, our optogenetic stimulation of Nts^{Cre} excitatory interneurons may have bypassed this inhibition, thereby shifting the balance of activity in favor of excitation, leading to an increase in the prevalence of wind-up.

Our data suggest that reverberatory activity within a neural circuit contributes to wind-up lamina I SPB neurons. It has long been speculated that interconnectivity among excitatory interneurons may provide a substrate for reverberatory activity, allowing for summation.²² Under physiological conditions, this summation is limited by activity in inhibitory interneurons, as evidenced by the observation that disinhibition by γ -aminobutyric acid and glycine antagonists causes long-lasting EPSCs by DRS.^{4,10,27,42} Thus, inhibition may normally limit wind-up. Because a decrease in inhibitory tone is frequently seen on injury,^{19,24} this loss of inhibition may contribute to abnormal reverberatory activity, giving rise to both heightened wind-up and abnormally elevated wind-up that are observed in pathological conditions.¹⁸

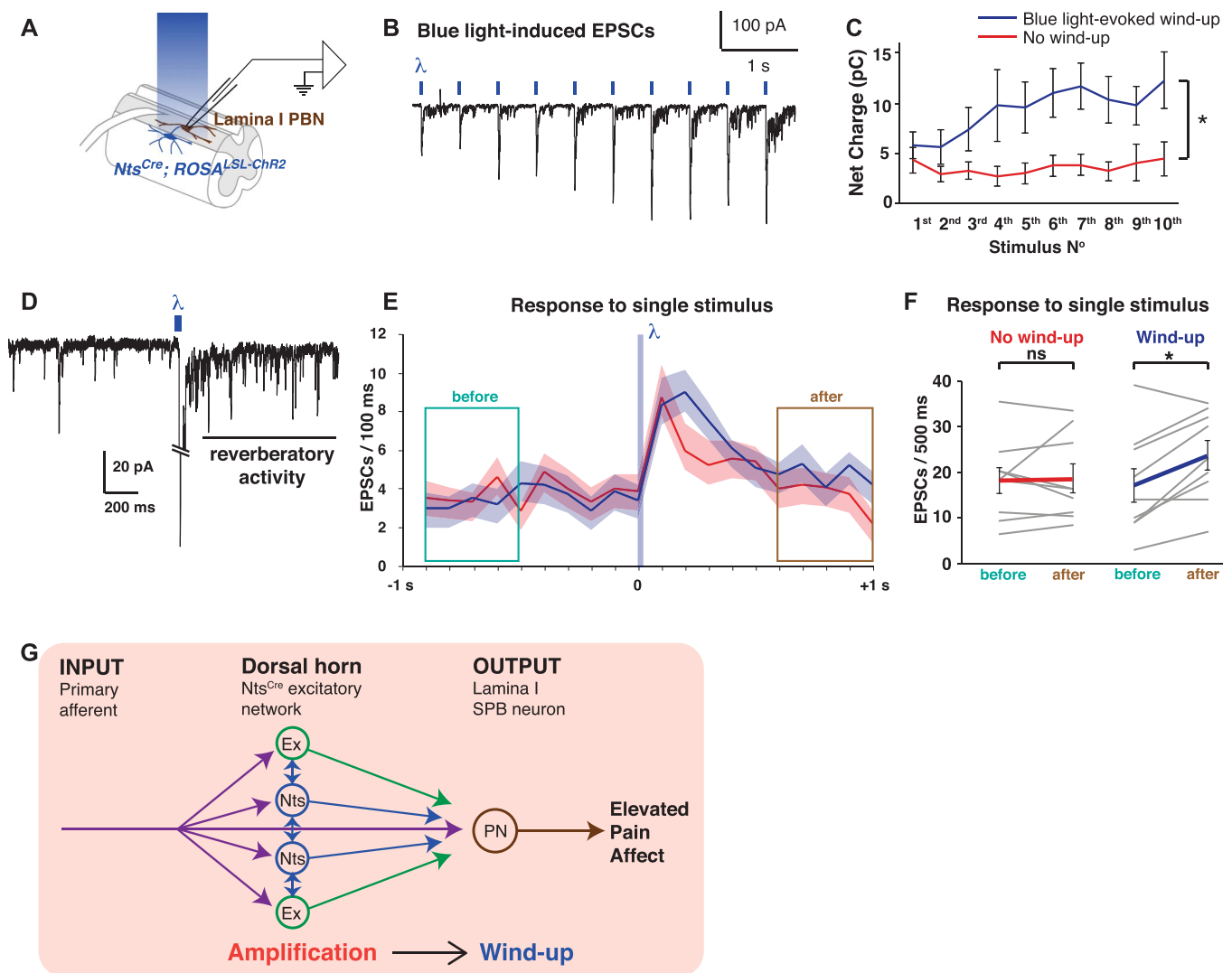


Figure 6. Activation of *Nts^{Cre}* neurons causes reverberatory activity that correlates with wind-up. (A) Diagram illustrating blue light stimulation of *Nts^{Cre}; ROSA26^{LSL-ChR2}* neurons during whole-cell patch-clamp recording from the lamina I SPB neurons. (B) Blue light stimulation at 2 Hz resulted in an increase of EPSCs in an SPB neuron that showed wind-up. (C) In SPB neurons that show wind-up, there is a frequency-dependent increase in net charge onto the recorded cell (ie, area under the curve) of each stimulation, which is significantly different than that observed in lamina I SPB neurons that do not undergo wind-up. Data are mean \pm SEM ($n = 11$ and 7 cells for blue light-evoked wind-up and no wind-up, respectively; * $P < 0.05$, 2-way ANOVA). (D) Single blue light stimulation (5 ms) of *Nts^{Cre}* neurons evoked persistent EPSCs in a lamina I PBN, indicative of reverberatory activity. (E) EPSCs in lamina I PBN neurons observed before (green box) or after (brown box) a single stimulation (5 ms) of *Nts^{Cre}* neurons with blue light. Lamina I SPB neurons that subsequently showed wind-up are shown in blue ($n = 9$); those that showed no wind-up are in red ($n = 9$). Data are mean \pm SEM. (F) A comparison of the number of EPSCs 1000 to 500 ms before optogenetic stimulation (green box in E) with that 500 to 1000 ms after optogenetic stimulation (brown box in E). In lamina I SPB neurons that do not show wind-up, there is no significant change in the number of EPSCs before and after a single optogenetic stimulus (red), whereas in lamina I neurons that do show wind-up, the number of EPSCs after optogenetic stimulation is significantly greater than before (blue). Data from individual neurons as well as mean \pm SEM are shown ($n = 9$; * $P < 0.05$, Student *t* test). (G) Model: during wind-up, primary afferent input is amplified by a network of excitatory *Nts^{Cre}* interneurons that synapse onto each other as well and other excitatory interneurons (Ex), thereby generating reverberatory activity, which contributes to wind-up in lamina I SPB neurons. ANOVA, analysis of variance; EPSC, excitatory postsynaptic current; PBN, parabrachial nucleus; PN, projection neuron; SPB, spinoparabrachial.

Conflict of interest statement

The authors have no conflict of interest to declare.

Research reported in this publication was supported by the National Institute of Arthritis and Musculoskeletal and Skin Diseases of the National Institutes of Health under Award Number R01 AR063772 and R21 AR064445 to S.E. Ross; the National Institute of Neurological Disorder and Stroke under Award Number NS023725 and NS096705 to H.R. Koerber, NS083347 to M.S. Gold, and NS096860 to M.M. Chiang; and the National Institutes of Diabetes and Digestive and Kidney Diseases under Award Number DK107966 to M.S. Gold. Part of this work was supported by a grant from the Rita Allen Foundation to S.E. Ross who is a Rita Allen Foundation Pain Scholar.

Article history:

Received 6 November 2017

Received in revised form 25 January 2018

Accepted 20 February 2018

Available online 23 March 2018

References

- Andrew D, Greenspan JD. Peripheral coding of tonic mechanical cutaneous pain: comparison of nociceptor activity in rat and human psychophysics. *J Neurophysiol* 1999;82:2641–8.
- Arendt-Nielsen L, Petersen-Felix S. Wind-up and neuroplasticity: is there a correlation to clinical pain? *Eur J Anaesthesiol Suppl* 1995; 10:1–7.

- [3] Arendt-Nielsen L, Petersen-Felix S, Fischer M, Bak P, Bjerring P, Zbinden AM. The effect of N-methyl-D-aspartate antagonist (ketamine) on single and repeated nociceptive stimuli: a placebo-controlled experimental human study. *Anesth Analg* 1995;81:63–8.
- [4] Baba H, Ji RR, Kohno T, Moore KA, Ataka T, Wakai A, Okamoto M, Woolf CJ. Removal of GABAergic inhibition facilitates polysynaptic A fiber-mediated excitatory transmission to the superficial spinal dorsal horn. *Mol Cell Neurosci* 2003;24:818–30.
- [5] Bourgeois L, Gauriau C, Monconduit L, Villanueva L, Bernard JF. Dendritic domains of nociceptive-responsive parabrachial neurons match terminal fields of lamina I neurons in the rat. *J Comp Neurol* 2003;464:238–56.
- [6] Cheng L, Arata A, Mizuguchi R, Qian Y, Karunaratne A, Gray PA, Arata S, Shirasawa S, Bouchard M, Luo P, Chen CL, Busslinger M, Goulding M, Onimaru H, Ma Q. Tlx3 and Tlx1 are post-mitotic selector genes determining glutamatergic over GABAergic cell fates. *Nat Neurosci* 2004;7:510–17.
- [7] Davies SN, Lodge D. Evidence for involvement of N-methylaspartate receptors in “wind-up” of class 2 neurones in the dorsal horn of the rat. *Brain Res* 1987;424:402–6.
- [8] Dickenson AH. A cure for wind up: NMDA receptor antagonists as potential analgesics. *Trends Pharmacol Sci* 1990;11:307–9.
- [9] Dickenson AH, Sullivan AF. Evidence for a role of the NMDA receptor in the frequency dependent potentiation of deep rat dorsal horn nociceptive neurones following C fibre stimulation. *Neuropharmacology* 1987;26:1235–8.
- [10] Duan B, Cheng L, Bourane S, Britz O, Padilla C, Garcia-Campmany L, Krashes M, Knowlton W, Velasquez T, Ren X, Ross S, Lowell BB, Wang Y, Goulding M, Ma Q. Identification of spinal circuits transmitting and gating mechanical pain. *Cell* 2014;159:1417–32.
- [11] Eide PK. Wind-up and the NMDA receptor complex from a clinical perspective. *Eur J Pain* 2000;4:5–15.
- [12] Eide PK, Jorum E, Stenehjem AE. Somatosensory findings in patients with spinal cord injury and central dysaesthesia pain. *J Neurol Neurosurg Psychiatry* 1996;60:411–15.
- [13] Eide PK, Jorum E, Stubhaug A, Bremnes J, Breivik H. Relief of post-herpetic neuralgia with the N-methyl-D-aspartic acid receptor antagonist ketamine: a double-blind, cross-over comparison with morphine and placebo. *PAIN* 1994;58:347–54.
- [14] Gauriau C, Bernard JF. Pain pathways and parabrachial circuits in the rat. *Exp Physiol* 2002;87:251–8.
- [15] Gutierrez-Mecinas M, Furuta T, Watanabe M, Todd AJ. A quantitative study of neurochemically defined excitatory interneuron populations in laminae I-III of the mouse spinal cord. *Mol Pain* 2016;12:1744806916629065.
- [16] Hachisuka J, Baumbauer KM, Omori Y, Snyder LM, Koerber HR, Ross SE. Semi-intact ex vivo approach to investigate spinal somatosensory circuits. *Elife* 2016;5:e22866.
- [17] Hedo G, Laird JM, Lopez-Garcia JA. Time-course of spinal sensitization following carrageenan-induced inflammation in the young rat: a comparative electrophysiological and behavioural study in vitro and in vivo. *Neuroscience* 1999;92:309–18.
- [18] Herrero JF, Laird JM, Lopez-Garcia JA. Wind-up of spinal cord neurones and pain sensation: much ado about something? *Prog Neurobiol* 2000;61:169–203.
- [19] Koerber HR, Brown PB. Quantitative analysis of dorsal horn cell receptive fields following limited deafferentation. *J Neurophysiol* 1995;74:2065–76.
- [20] Koltzenburg M, Handwerker HO. Differential ability of human cutaneous nociceptors to signal mechanical pain and to produce vasodilatation. *J Neurosci* 1994;14:1756–65.
- [21] Lundberg LE, Jorum E, Holm E, Torebjork HE. Intra-neural electrical stimulation of cutaneous nociceptive fibres in humans: effects of different pulse patterns on magnitude of pain. *Acta Physiol Scand* 1992;146:41–8.
- [22] Mendell LM. Physiological properties of unmyelinated fiber projection to the spinal cord. *Exp Neurol* 1966;16:316–32.
- [23] Mendell LM, Wall PD. Responses of single dorsal cord cells to peripheral cutaneous unmyelinated fibres. *Nature* 1965;206:97–9.
- [24] Moore KA, Kohno T, Karchewski LA, Scholz J, Baba H, Woolf CJ. Partial peripheral nerve injury promotes a selective loss of GABAergic inhibition in the superficial dorsal horn of the spinal cord. *J Neurosci* 2002;22:6724–31.
- [25] Nakatsuka T, Park JS, Kumamoto E, Tamaki T, Yoshimura M. (1999). Plastic changes in sensory inputs to rat substantia gelatinosa neurons following peripheral inflammation. *Pain* 1999;82:39–47.
- [26] Nikolajsen L, Hansen CL, Nielsen J, Keller J, Arendt-Nielsen L, Jensen TS. The effect of ketamine on phantom pain: a central neuropathic disorder maintained by peripheral input. *PAIN* 1996;67:69–77.
- [27] Peirs C, Williams SP, Zhao X, Walsh CE, Gedeon JY, Cagle NE, Goldring AC, Hioki H, Liu Z, Marell PS, Seal RP. Dorsal horn circuits for persistent mechanical pain. *Neuron* 2015;87:797–812.
- [28] Pinto V, Szucs P, Derkach VA, Safronov BV. Monosynaptic convergence of C- and Adelta-afferent fibres from different segmental dorsal roots on to single substantia gelatinosa neurones in the rat spinal cord. *J Physiol* 2008;586:1165–77.
- [29] Pinto V, Szucs P, Lima D, Safronov BV. Multisegmental A(delta)- and C-fiber input to neurons in lamina I and the lateral spinal nucleus. *J Neurosci* 2010;30:2384–95.
- [30] Price DD. Characteristics of second pain and flexion reflexes indicative of prolonged central summation. *Exp Neurol* 1972;37:371–87.
- [31] Price DD, Long S, Huitt C. Sensory testing of pathophysiological mechanisms of pain in patients with reflex sympathetic dystrophy. *PAIN* 1992;49:163–73.
- [32] Price DD, Mao J, Frenk H, Mayer DJ. The N-methyl-D-aspartate receptor antagonist dextromethorphan selectively reduces temporal summation of second pain in man. *PAIN* 1994;59:165–74.
- [33] Punnakal P, von Schoultz C, Haenraets K, Wildner H, Zeilhofer HU. Morphological, biophysical and synaptic properties of glutamatergic neurons of the mouse spinal dorsal horn. *J Physiol* 2014;592:759–76.
- [34] Safronov BV, Pinto V, Derkach VA. High-resolution single-cell imaging for functional studies in the whole brain and spinal cord and thick tissue blocks using light-emitting diode illumination. *J Neurosci Methods* 2007;164:292–98.
- [35] Sarlani E, Grace EG, Reynolds MA, Greenspan JD. Sex differences in temporal summation of pain and after sensations following repetitive noxious mechanical stimulation. *PAIN* 2004;109:115–23.
- [36] Schouenborg J, Sjolund BH. Activity evoked by A- and C-afferent fibers in rat dorsal horn neurons and its relation to a flexion reflex. *J Neurophysiol* 1983;50:1108–21.
- [37] Smith KM, Boyle KA, Madden JF, Dickinson SA, Jobling P, Callister RJ, Hughes DI, Graham BA. Functional heterogeneity of calcitonin-expressing neurons in the mouse superficial dorsal horn: implications for spinal pain processing. *J Physiol* 2015;593:4319–39.
- [38] Smith KM, Boyle KA, Mustapa M, Jobling P, Callister RJ, Hughes DI, Graham BA. Distinct forms of synaptic inhibition and neuromodulation regulate calcitonin-positive neuron excitability in the spinal cord dorsal horn. *Neuroscience* 2016;326:10–21.
- [39] Szucs P, Pinto V, Safronov BV. (2009). Advanced technique of infrared LED imaging of unstained cells and intracellular structures in isolated spinal cord, brainstem, ganglia and cerebellum. *J Neurosci Methods* 2009;177:369–80.
- [40] Thompson SW, Dray A, McCarron KE, Krause JE, Urban L. Nerve growth factor induces mechanical allodynia associated with novel A fibre-evoked spinal reflex activity and enhanced neurokinin-1 receptor activation in the rat. *PAIN* 1995;62:219–31.
- [41] Thompson SW, King AE, Woolf CJ. Activity-dependent changes in rat ventral horn neurons in vitro; summation of prolonged afferent evoked postsynaptic depolarizations produce a d-2-amino-5-phosphonovaleric acid sensitive windup. *Eur J Neurosci* 1990;2:638–49.
- [42] Torsney C, MacDermott AB. Disinhibition opens the gate to pathological pain signaling in superficial neurokinin 1 receptor-expressing neurons in rat spinal cord. *J Neurosci* 2006;26:1833–43.
- [43] Traub RJ. Spinal modulation of the induction of central sensitization. *Brain Res* 1997;778:34–42.
- [44] Vase L, Svensson P, Nikolajsen L, Arendt-Nielsen L, Jensen TS. The effects of menthol on cold allodynia and wind-up-like pain in upper limb amputees with different levels of phantom limb pain. *Neurosci Lett* 2013;534:52–7.
- [45] Vierck CJ Jr, Cannon RL, Fry G, Maixner W, Whitsel BL. Characteristics of temporal summation of second pain sensations elicited by brief contact of glabrous skin by a preheated thermode. *J Neurophysiol* 1997;78:992–1002.
- [46] Warncke T, Stubhaug A, Jorum E. Ketamine, an NMDA receptor antagonist, suppresses spatial and temporal properties of burn-induced secondary hyperalgesia in man: a double-blind, cross-over comparison with morphine and placebo. *PAIN* 1997;72:99–106.
- [47] Woolf CJ. Windup and central sensitization are not equivalent. *PAIN* 1996;66:105–8.
- [48] Woolf CJ, Thompson SW. The induction and maintenance of central sensitization is dependent on N-methyl-D-aspartic acid receptor activation; implications for the treatment of post-injury pain hypersensitivity states. *PAIN* 1991;44:293–9.
- [49] Woolf CJ, Wall PD. Relative effectiveness of C primary afferent fibers of different origins in evoking a prolonged facilitation of the flexor reflex in the rat. *J Neurosci* 1986;6:1433–42.
- [50] Zhang DX, Owens CM, Willis WD. Intracellular study of electrophysiological features of primate spinothalamic tract neurons and their responses to afferent inputs. *J Neurophysiol* 1991;65:1554–66.